ACS SyntheticBiology

Research Article

pubs.acs.org/synthbio

Effects of Compartment Size on the Kinetics of Intracompartmental Multimeric Protein Synthesis

Tomoaki Matsuura,[†,∥] Kazufumi Hosoda,[§] Yasuaki Kazuta,[∥] Norikazu Ichihashi,[∥] Hiroaki Suzuki,[∥,§] and Tetsuya Yomo*[,∥,‡,§]

[†]Department of Biotechnology, Graduate School of Engineering, [‡]Graduate School of Frontier Biosciences, and [§]Department of Bioinformatic Engineering, Graduate School of Information Science and Technology, Osaka University, Yamadaoka 1-5, Suita, Osaka, Japan

[∥]Exploratory Research for Advanced Technology, Japan Science and Technology Agency, Yamadaoka 1-5, Suita, Osaka, Japan

Supporting Information

ABSTRACT: The cell contents are encapsulated within a compartment, the volume of which is a fundamental physical parameter that may affect intracompartmental reactions. However, there have been few studies to elucidate whether and how volume changes alone can affect the reaction kinetics. It is difficult to address these questions *in vivo*, because forced cell volume changes, e.g., by osmotic inflation/deflation, globally alters the internal state. Here, we prepared artificial cell-like compartments with different volumes but with identical constituents, which is not possible with living cells, and synthesized two tetrameric enzymes, *β*-glucuronidase (GUS) and *β*-galactosidase (GAL), by cell-free protein synthesis. Tetrameric GUS but not GAL was synthesized more quickly in smaller compartments. The difference between the two was dependent on the rate-limiting step and the reaction order. The observed acceleration mechanism would be applicable to living cells as multimeric protein synthesis in a microcompartment is ubiquitous *in vivo*.

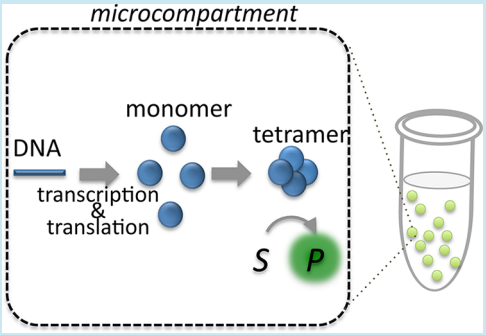

KEYWORDS: *microcompartment, compartmentalization, PURE system, water-in-oil emulsion, protein synthesis*

The cell contents are encapsulated within a compartment, the volume of which is a fundamental physical parameter. Cells change their shape and volume during the cell cycle and in response to the external environment, such as osmotic stress or the presence of certain compounds.[1−4] Indeed, it has been elucidated how the intracellular reactions, including gene expression, cellular metabolism, and signaling systems, are altered in association with changes in cell size and shape *in vivo*.[5−8] Meanwhile, as the cell volume serves as the physical constraint for all cytosolic components, cell volume itself may exert effects on intracellular reactions.[9,10] However, when the cell is viewed as a simple chemical and physical system, it remains unclear how differences in volume alone affect the kinetics of intracompartmental reactions. Are there biochemical reactions that are affected in response to changes solely in compartment volume? In addition, if they do indeed exist, what is the mechanism underlying transmission of volume change directly to such intracompartmental reactions? As forcing changes in cell volume typically by osmotic inflation/deflation globally alters the internal state of the cell,[11,12] it is difficult to address these fundamental questions by *in vivo* studies.

Complex biochemical reactions, including protein translation,[13] oscillatory circuits,[14] self-replication,[15] and circadian rhythm,[16] have been isolated from the cell and constructed *in vitro* from purified and defined components to gain a deeper understanding of the biochemical reactions from the molecular to the system level. Moreover, because cells are spatially bounded by the cell membrane, biological reactions, such as nucleotide polymerization,[17−19] protein translation,[20−24] membrane protein translocation,[25] and self-replication,[26,27] have been modeled in vesicular compartments. Unlike *in vivo* studies, such reconstituted systems are free from unknown components, and their composition can be designed as desired, which facilitates obtaining a systematic and comprehensive understanding of the complex chemical reaction.[28−30] Here, we used *in vitro* synthetic biology approach to elucidate how the biochemical reaction may be affected solely by the volume of the compartment where the reactions occur.

The present study was performed to create artificial compartments with different volumes containing the components necessary for transcription and translation cascade reactions to investigate the effects of compartment volume alone on these indispensable reactions. We first developed microcompartments using water-in-oil (w/o) emulsion droplets[31,32] encapsulating an *in vitro* transcription and translation (IVTT) system,[33,34] where the reaction volume can be changed as an experimental parameter. *β*-Glucuronidase (GUS) or *β*-galactosidase (GAL), both tetrameric enzymes, were synthe-

Received: April 28, 2012
Published: July 3, 2012

sized using the IVTT inside microcompartments of different volumes ranging from 43 fL to 2 μL. We found that tetrameric GUS was synthesized earlier with decreasing compartment volume, but no such acceleration was observed for GAL. The kinetic mechanism underlying the difference in dependence of tetrameric enzyme synthesis with regard to compartment volume was identified.

RESULTS AND DISCUSSION

The responses of intracellular state and reactions to cell size have attracted considerable attention. Simple phenomena, such as diffusive mixing, molecular transport, and enzymatic reactions, in physically confined spaces have been studied experimentally and theoretically in biological contexts,[9,10] but the effects on highly complex cascade reactions, which are ubiquitous in cells, have not been discussed in sufficient detail. In the present study, we prepared artificial cell-like compartments with different volumes but with identical constituents, which is not possible with living cells, and investigated the effects of compartment volume on the cascade reaction of transcription, translation, and tetramer assembly.

Detecting Synthesis of Tetrameric GUS and GAL in Microcompartments. We used droplets of a water-in-oil (w/o) emulsion as microcompartments and encapsulated a reconstituted *in vitro* transcription/translation system (IVTT), the PURE system,[13,35] together with the DNA encoding the reporter protein β-glucuronidase (GUS) or β-galactosidase (GAL)[36−38] (Figure 1a). GUS and GAL are tetrameric enzymes that assemble into tetramers,[39,40] the only form exhibiting catalytic activity, starting from monomer to dimer, followed by dimer to tetramer (Supplementary Figure 1). We previously investigated the kinetics of tetramerization of these enzymes when coupled with protein translation using the IVTT in a test tube[41] and found that the assembly rate constant of GAL is approximately 1000-fold larger than that of GUS (i.e., on the order of 10^2 and 10^5 M^{-1} s^{-1} with GUS and GAL, respectively). The present study was performed to investigate the behavior of these two different reactions when encapsulated in microcompartments of different volumes.

We prepared w/o emulsions with different volumes (Figure 1a,b). Briefly, 2 μL of IVTT reaction mixture was dispersed into 200 μL of oil, and by altering the mixing strategy emulsion droplets of three different sizes were prepared, resulting in average volumes of 43 fL, 9.1 pL, and 2 μL (designated as Se, Me, and Le, respectively) (Figure 1b,c). Le was prepared by gently adding the mixture to the oil phase, resulting in a single water droplet of 2 μL. Me was prepared by vigorously mixing the solution using a vortex mixer. Se was prepared by passing the solution through a porous membrane. GUS and GAL syntheses were performed in the presence of their fluorogenic substrates (FDGlcU and FDG, respectively). Therefore, when the tetrameric enzyme was assembled from monomers produced through transcription and translation, the fluorogenic substrate was hydrolyzed, resulting in the production of fluorescein. The synthesis of two enzymes, i.e., tetrameric GUS and GAL, inside the compartment could be detected in real-time as an increase in the green fluorescence signal (Figure 1a).

Preparation Method and Surface Properties of the Microcompartments Do Not Affect Intracompartmental Enzyme Synthesis. As described above, different strategies were used to prepare IVTT-containing droplets with different volumes. In addition, because smaller microcompartments have higher surface-to-volume ratios, the inner solution experiences a greater effective detergent concentration. These properties may have an inhibitory effect on enzyme synthesis. We examined whether the surface properties or the preparation method affects the intracompartmental reaction. We first found that simple substrate hydrolysis with purified tetrameric GUS enzyme proceeded similarly irrespective of the compartment volume (Supplementary Figure 2). Second, GUS and GAL syntheses were performed with 1 nM DNA, and the time courses of changes in fluorescence intensity of the entire reaction mixture (2 μL) were measured (Figure 2a). At this concentration, a single compartment of Se, Me, and Le emulsions contained on average 10^9, 5460, and 26 copies of DNA, respectively (Supplementary Table 1). The results in each volume were almost identical to each other (Figure 2a). These results suggested that GUS and GAL syntheses are hardly affected by the preparation method or the surface properties of the microcompartments.

Synthesis of Tetrameric GUS at Lower DNA Concentration Is Accelerated in Smaller Microcompartments. We next investigated the effects of compartment volume on the syntheses of tetrameric GUS and GAL at lower DNA concentrations (Supplementary Table 2). GUS and GAL syntheses were carried out in Le, Me, or Se emulsions at DNA concentrations of 1, 0.3, 0.1, 0.03, 0.01, or 0.003 nM, and the time courses of changes in fluorescence intensity of the entire reaction mixture (2 μL) are shown in Figure 2a,d. Only

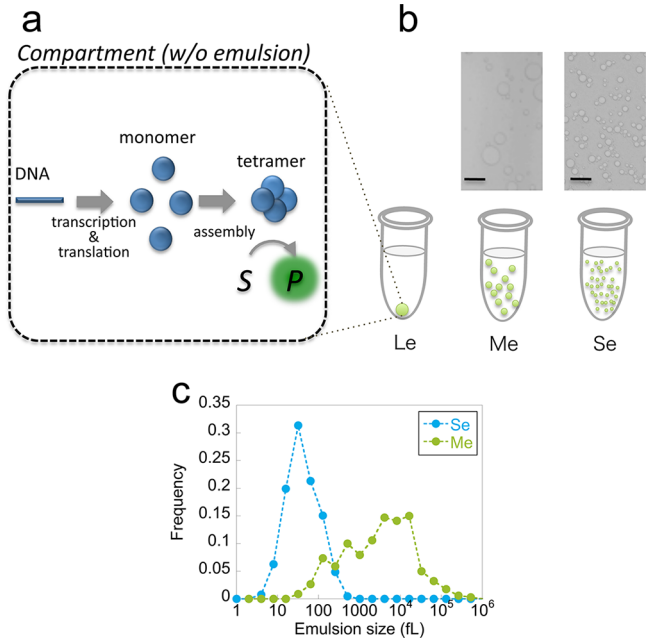

Figure 1. Schematic of GUS and GAL syntheses in water-in-oil (w/o) emulsion droplets of different volumes. (a) GUS and GAL syntheses within the emulsions were detected through a reaction cascade consisting of transcription, translation, monomer-to-tetramer assembly, and fluorescent substrate hydrolysis. (b) Schematic and microscopic images of the three compartments used in this study. Scale bar indicates 20 μm. (c) Volume distributions of Me and Se. The volumes of more than 1000 droplets were evaluated from microscopic images, assuming droplets were spherical. Se and Me had mean volumes of 43 fL and 9.1 pL, respectively. Detailed statistics are given in Supplementary Table 3. Note that the compartment volume and/or preparation method had only minimal effects on the enzymatic reaction or fluorescent signal (Supplementary Figure 2).

dx.doi.org/10.1021/sb300041z | ACS Synth. Biol. 2012, 1, 431−437

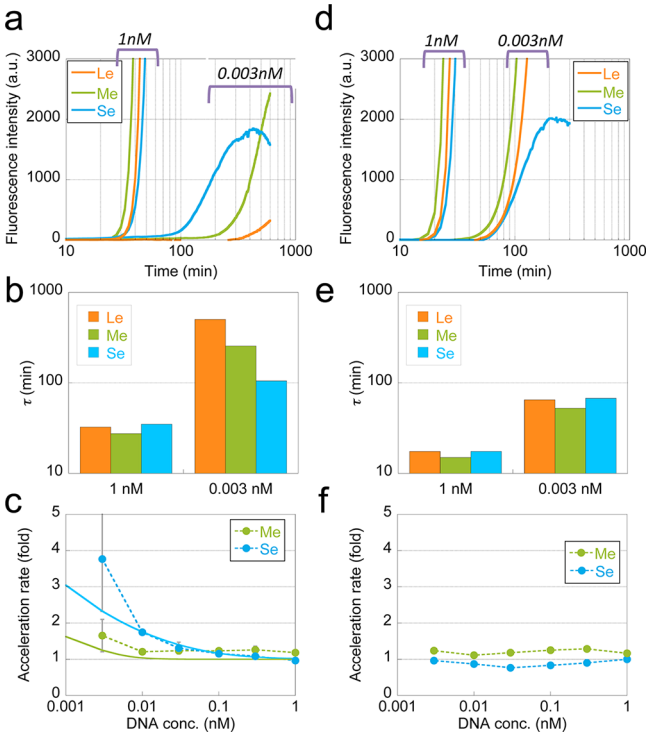

Figure 2. Time courses of GUS and GAL syntheses. Representative data for (a) GUS and (d) GAL syntheses in compartments of three different volumes (Se (43 fL), Me (9.1 pL), and Le (2 μL)) are shown. The DNA concentrations were 1, 0.3, 0.1, 0.03, 0.01, and 0.003 nM. The results with 1 nM and 0.003 nM DNA are shown (other results are shown in Supplementary Figure 3). (b, e) Lag time t for the reactions at different compartment volumes, obtained from the data shown in panels a and d using 1 nM or 0.003 nM DNA encoding (b) GUS or (e) GAL. τ is the time required to reach a threshold fluorescence intensity of 200 (au). The threshold is defined as the fluorescent signal that is sufficient to exceed the detection limit but small enough to permit the effect of substrate depletion to be neglected. Supplementary Figure 5 summarizes all of the data on the relationship between DNA concentration and τ. (c, f) Relationship between DNA concentration and acceleration rate (Ar, eq 1) of (c) GUS and (f) GAL syntheses. The results in panel c are the means ±1 SE of two independent experiments. The green and blue lines show the theoretical curves given by eq 2 for Me and Se, respectively.

the data for 1 and 0.003 nM DNA are shown for clarity, and those for other DNA concentrations are presented in Supplementary Figure 3. As described above, GUS and GAL syntheses at 1 nM DNA showed similar results irrespective of the compartment volume. On the other hand, a large variation in the time course among the compartment volumes was seen with 0.003 nM GUS DNA; the fluorescence signal started to increase more quickly in smaller compartments (Figure 2a). For GAL, the fluorescence signal started to increase with a similar timing in different compartments even at 0.003 nM DNA (Figure 2d). The rate of the increase in fluorescence signal d[FI]/dt is linearly related to the tetramer concentration, and thus the earlier increase in the fluorescence signal indicated the earlier production of tetramer. Therefore, the results shown in Figure 2a,d indicated that the behavior of tetrameric enzyme synthesis in smaller compartments was different between GUS and GAL. Note that, despite different dynamics, in Se at 0.003 nM DNA, the fluorescence signals for GUS and GAL synthesis reached the same plateaus at values much lower than that obtained when the fluorogenic substrate was fully hydrolyzed.

To analyze these observations more quantitatively, we defined the acceleration rate $\mathrm{Ar}_d^{\mathrm{X}}$ in X emulsion (where X denotes size, either Me or Se) at DNA concentration d as

$$\mathrm{Ar}_d^{\mathrm{X}} = \tau_d^{\mathrm{Le}}/\tau_d^{\mathrm{X}} \quad (1)$$

where τ_d^{X} is the lag time, i.e., the time required to reach a fluorescence intensity of 200 (au), which is far below the signal obtained when the fluorogenic substrate was fully hydrolyzed (~30000) (Figure 2b,e). Thus, the acceleration rate represents how fast the fluorescence intensity in Me or Se emulsions reached a threshold compared to Le. That is, $\mathrm{Ar}_d^{\mathrm{X}}$ became larger than 1 when the synthesis of tetrameric enzymes in Se or Me was faster than that in Le at identical DNA concentration. $\mathrm{Ar}_d^{\mathrm{X}}$ was estimated for all DNA concentrations tested. Figure 2c,f shows the relationship between Ar and the DNA concentrations of GUS and GAL, respectively. GUS showed increased Ar values for smaller d (Figure 2c), while GAL had a value of approximately 1 irrespective of the DNA concentration and compartment volume (Figure 2f). Thus, tetrameric GUS synthesis, but not that of GAL, was accelerated in smaller droplets, and this effect was pronounced at lower DNA concentrations.

Mechanism of the Acceleration of Tetrameric GUS Synthesis in Smaller Compartments. What is the reason for the substantial acceleration of synthesis of tetrameric GUS in Se compared to Le? We hypothesized that the acceleration occurs when a cell mimetic condition is achieved, i.e., nearly a single copy of DNA is encapsulated in a micrometer-size compartment (Figure 3a). We dispersed 2 μL of the reaction mixture in oil to prepare the emulsions. When the initial DNA concentration becomes extremely low such that the number of DNA molecules is less than the number of compartments and that the number of DNA encapsulated in each compartment follows a Poisson distribution, most of the compartments that have DNA carry nearly a single copy (Figure 3a, step I). In a compartment with a single copy of the DNA, the effective DNA concentration becomes greater than that in larger compartments (Supplementary Table 1). Similarly, the monomers translated from a single DNA are more concentrated in small than in large compartments (Figure 3a, step II). As a result of such "condensation," the rate of tetramer assembly is also increased (step III), leading to the rapid appearance of green fluorescence (Ar > 1 (Figure 2c)). Such condensation will not occur at DNA concentrations at which DNA is present in all compartments, e.g., d > 0.1 nM (Supplementary Table 2), so an Ar ≈ 1 above 0.1 nM DNA is reasonable (Figure 2c).

If the above hypothesis is correct, only a fraction of the compartments, in which a copy of DNA is encapsulated, should exhibit green fluorescence at a low DNA concentration, as depicted in Figure 3a (step IV) (Supplementary Figure 4). This was indeed the case as confirmed by fluorescence microscopy (Figure 3b). The plateaus observed with both GUS and GAL at 0.003 nM DNA (Figure 2a,d) were consistent with the observation that DNA is encapsulated in a fraction of the droplets. Furthermore, when incubating the reaction mix until the fluorogenic substrate was completely hydrolyzed (step IV in Figure 3a), the fluorescence intensity of the entire reaction mixture in Se should become smaller with decreasing DNA concentration, while nearly identical values should be obtained for Le and Me as there are very few compartments without DNA (Supplementary Figure 4). Our results agreed well with these predictions (Figure 3c).

dx.doi.org/10.1021/sb300041z | ACS Synth. Biol. 2012, 1, 431–437

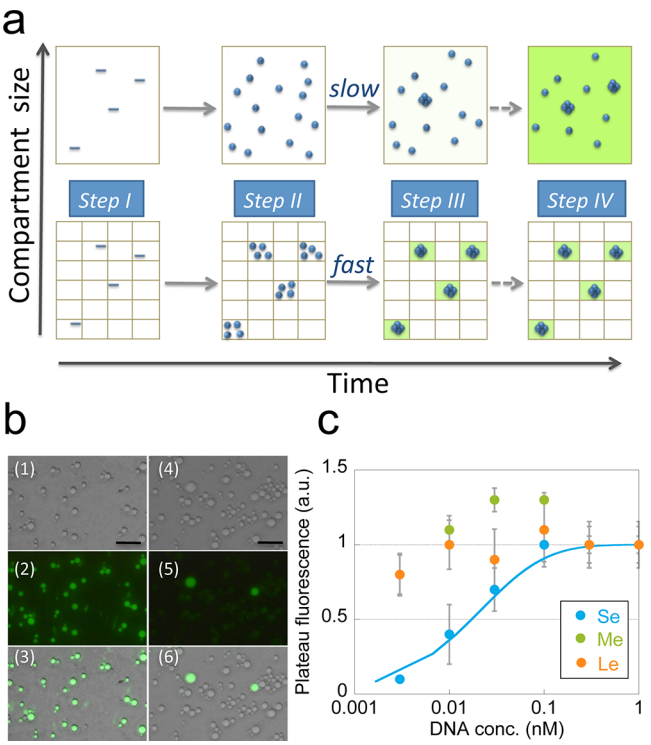

Figure 3. Schematic for the mechanism of GUS synthesis acceleration in small vs large compartments. (a) Step I: First, identical numbers of DNA molecules were encapsulated into compartments of different volumes. Note that the total volume was the same between the two. Step II: Identical numbers of monomers were synthesized through transcription and translation of each DNA molecule, irrespective of the compartment volume. Step III: The numbers of tetramers synthesized were larger in the smaller compartment because the monomer concentration was higher than in the larger compartment. As GUS is active only when it tetramerizes, the fluorescent product appeared earlier in the smaller compartment. Step IV: After a sufficient period, all of the fluorescent substrate present in the compartment that contains DNA was hydrolyzed. All of the fluorescent substrate was hydrolyzed in large compartments, whereas only a portion of the substrate was hydrolyzed in small compartments. (b) (1, 4) Bright field, (2, 5) fluorescence, and (3, 6) merged images of Se with (1, 2, 3) 0.3 nM or (4, 5, 6) 0.01 nM DNA after 20-h reaction period. Scale bar indicates 20 μm. (c) Relationship between DNA concentration and fluorescence intensity after a 20-h reaction period. The fluorescence of each emulsion with 1 nM DNA was defined as 1. The results shown are the means ±1 SE of two independent experiments. The line shows the theoretical curve given by eq 3.

Note that the encapsulation of the components of the IVTT is unlikely to affect the acceleration of GUS synthesis. The component with the lowest concentration in the IVTT used here was nucleoside diphosphate kinase (NDK), which was present at 16 nM.[42] At this concentration, Se would hold on average 413 NDK molecules. Therefore, even NDK should have much smaller variation comparing to that of DNA in all droplets (cv <5%).

Mechanism Underlying the Lack of Acceleration of Tetrameric GAL Synthesis in Smaller Compartments. The above describes the reasons for the acceleration of tetrameric GUS synthesis, but why is such acceleration not observed with GAL? With both GUS and GAL DNA in Se at a DNA concentration of 0.003 nM, nearly a single copy of DNA is encapsulated in each droplet, which can be seen from the time course data in Figure 2a,d, showing that the fluorescence signal quickly reaches a plateau. What is the difference between GUS and GAL, and what are the prerequisites for a reaction to be affected by the compartment volume?

The difference between GUS and GAL can be described by the difference in the rate-limiting step of the reaction. We reported previously that at similar concentrations the assembly of tetrameric GAL from monomers occurs much faster than that of tetrameric GUS when coupled to protein translation using the IVTT employed in this study.[41] The rate-limiting step was identified as monomer-to-tetramer assembly for tetrameric GUS, whereas those for tetrameric GAL synthesis were the transcription and translation steps. Let us assume that the compartment volume does not affect monomeric protein synthesis, which is the case with our experimental setup (Figure 2a,d, data with 1 nM DNA), i.e., a defined number of monomers are synthesized through transcription and translation per DNA irrespective of the compartment volume. At the assembly stage, the stage between Step II and Step III in Figure 3a, tetrameric GUS is produced more quickly in smaller compartments as shown in Figure 3a because the rate-limiting step is monomer-to-tetramer assembly. On the other hand, tetrameric GAL is produced equally in both large and small compartments, because the assembly is so fast that monomers assemble into tetramers as soon as they are synthesized. Therefore, acceleration was observed with tetrameric GUS but not GAL.

Qualitative Evaluation of the Acceleration Mechanism. Above, we presented a qualitative explanation of the mechanism underlying acceleration of tetrameric GUS synthesis in small compartments, which is pronounced at lower DNA concentrations, and the reason why such acceleration is not observed with tetrameric GAL. In this section, we evaluate the observation quantitatively to further confirm that the hypothesis proposed above is appropriate to describe the data. For this purpose, we developed a mathematical model that describes multimeric protein synthesis in a microcompartment and compared the model with the experimental data.

The cascade reaction of transcription, translation, tetramer assembly, and fluorescence substrate hydrolysis (Supplementary Figure 1) was modeled in bulk and in droplets where the bulk solution was subdivided into w/o emulsions, to obtain the time evolution of the concentration of hydrolyzed product [P]. All equations and derivations are presented in the Supporting Information. Using these equations, we derived an equation that predicts the relationship between Ar and d of tetrameric GUS and GAL synthesis:

$$\mathrm{Ar}_d^{\mathrm{X}}(GUS) = \sqrt[12]{1 + \frac{\mu_{-2}}{\bar{v}}\cdot(d\cdot N_{\mathrm{A}})^{-3} + 7\frac{\mu_{-1}}{\bar{v}}(d\cdot N_{\mathrm{A}})^{-2} + \frac{6}{\bar{v}}(d\cdot N_{\mathrm{A}})^{-1}}$$

$$\mathrm{Ar}_d^{\mathrm{X}}(GAL) = 1 \qquad (2)$$

where μ_k is the kth moment of $p(v)$, probability density function of the emulsion droplet volume distribution, $\bar{v}$ is the average volume of the droplet and N_{A} is Avogadro's number. When the above equations were plotted together with the experimental data, both showed similar trends (Figure 2c,f). Note that the slight deviation of experimental data from theoretical prediction in Figure 2c could be caused by the approximation that the transcription/translation activity of the IVTT remains constant during the measurement (Supplemen-

dx.doi.org/10.1021/sb300041z | ACS Synth. Biol. 2012, 1, 431–437

tary Figure 5). Furthermore, we derived an equation that predicts the relationship between d and fluorescence intensity after complete substrate hydrolysis in Se:

$$\mathrm{pla} = 1 - \frac{1}{\bar{v}}\frac{1}{\sqrt{2\pi}S}\int_0^V \exp\left[\frac{-(\ln v - M)^2}{2S^2} - d{\cdot}v{\cdot}N_A\right]dv \quad (3)$$

where M and S are the average and standard deviation of the log-normal distribution $p(v)$ on a logarithmic scale. When the above equations were plotted together with the experimental data, both showed similar trends (Figure 3c). Note that there is no fitting parameter in these equations (eqs 2 and 3). The consistency between the model and the experimental data strongly supports the validity of the proposed mechanism (Figure 3a) of acceleration of tetrameric GUS synthesis and lack of acceleration of GAL synthesis.

GUS and GAL Synthesis Is a Fourth and First-Order Reaction, Respectively. We showed experimentally that the compartment volume alone can have a measurable effect on intracellular reactions using this artificially reconstructed system. Depending on the nature of the rate-limiting step, the compartment volume either does or does not affect multimeric protein synthesis. Tetrameric GUS and GAL synthesis differ not only in their rate-limiting step but also in their reaction order. While both reactions follow similar cascades, GUS and GAL synthesis follow fourth- and first-order reaction kinetics, respectively (Supplementary Figure 5).[41]

$$\frac{d(N_{GUS,tetramer}/v)}{dt} \propto (N_{DNA}/v)^4$$
$$\frac{d(N_{GAL,tetramer}/v)}{dt} \propto (N_{DNA}/v) \quad (4)$$

where $N_{GUS\_tetramer}$, $N_{GAL\_tetramer}$, and N_{DNA} represent the number of tetrameric GUS, GAL, and DNA molecules in a compartment with a volume of v, respectively. See Supporting Information for equations and derivations (eqs s2 and s3). Let us assume the presence of a single copy of DNA in a compartment where a defined number of monomers are synthesized per DNA. When the compartment volume was decreased (increased) by 2-fold, the rates of tetrameric GUS and GAL synthesis increased (decreased) by 8 (= $2^4/2$) or 1 (= $2^1/2$)-fold, respectively. With changes in compartment volume alone, the number of tetrameric GAL molecules synthesized does not change, whereas that of tetrameric GUS responds in a high-order manner and is therefore highly sensitive to small changes in compartment volume. High sensitivity of high-order reaction, not limited to multimeric enzyme synthesis, could be one of the fundamental strategies that cells use to switch gene expression, metabolic pathways, and signaling cascades on and off in response to changes in cell volume, although no such mechanisms have yet been demonstrated *in vivo*.

It is important to note that multimerization is a concentration-dependent reaction, and thus the gene expression level may affect the compartment volume dependency of multimeric protein synthesis. While we used GUS and GAL, both of which are homotetramers, the compartment volume can affect the formation of other complexes that are abundant in nature,[43] including hetero-oligomer synthesis, and complexes of RNA or DNA with proteins.

Conclusion. In previous studies, enhanced GFP synthesis by IVTT in a microcompartment has been observed, while the mechanism remains unclear.[44,45] Using an *in vitro* synthetic biology approach, we have shown that the compartment volume alone can affect intracompartmental multimeric protein synthesis and revealed its mechanism using a mathematical model. With cells, many parameters, including gene expression, metabolite transport, and membrane dynamics, are associated with change in the cell size, while with our experimental setup, we isolated the effect of altering the compartment volume from others, which enabled us to investigate the effect of changes in solely the compartment volume. Our system is very different from living cells, but the simplicity allows us to control various parameters and thus provides a platform to study how the compartment volume, one of the fundamental physical parameters of the cell, affects intracompartmental biological reaction networks.

Our work does not intend to clarify the effect of volume to a specific cell. Instead, we considered a hypothetical general "cell" that consists of intracellular reaction and microscale container and elucidated the relation between the compartment size and the multimeric protein synthesis. We think that the observed acceleration mechanism would be applicable generally, because synthesis and assembly of multimeric proteins as well as the micrometer to submicrometer compartments (plasma membranes and organelles) are ubiquitous in cells. In addition, acceleration mechanism must be taking into account when discussing the evolution of primitive cells[46,47] and for the construction of artificial cells.[30,48]

METHODS

***In Vitro* Transcription and Translation.** Plasmids encoding GAL and GUS (pET-lacZ and pET-gusA, respectively) were constructed as described previously.[42] A reconstituted *in vitro* transcription/translation (IVTT) system was used in this study (PURE system[13]) and was modified according to previous studies.[49,50] For GAL and GUS syntheses, template DNA (plasmid) was added to the IVTT and was supplemented with 4 units of RNasin (Promega) and the fluorescent substrate fluorescein di-β-D-galactopyranoside (FDG) or fluorescein di-β-D-glucuronide (FDGlcU) (Invitrogen) at a concentration of 50 μM. Neither FDG nor FDGlcU fluoresces before hydrolysis, but both yield fluorescein that emits green fluorescence as a result of hydrolysis.

Water-in-Oil (w/o) Emulsion Droplet Preparation. Detergent containing oil [2% Span 80, 1% Tween 80 and 2.5% ABIL-EM90 in decane, anhydrous (all from Sigma)] was first pretreated with saturation buffer [100 mM HEPES (pH 7.6), 280 mM potassium glutamate, 1.5 mM spermidine, 18 mM magnesium acetate, 25 mM creatine phosphate, 12 mM DTT, 0.01 μg/mL formic acid, 6% glycerol, and 0.1% BSA]. Briefly, 180 μL of saturation buffer was added to 1.5 mL of detergent containing oil, vortexed briefly, and then incubated for 20 min at 37 °C. The upper phase was collected after centrifugation at 22000 × g for 20 min at 4 °C. The collected saturated oil was used to prepare w/o emulsions; 2 μL of IVTT reaction mixture was added to 200 μL of presaturated oil, and the size was varied by the mixing strategy. Le (2 μL) was prepared by gently adding 2 μL of the IVTT reaction mixture to the oil phase, resulting in a single water droplet of 2 μL. Me (average 9.1 pL) was prepared by vigorously mixing the solution using a vortex mixer for 60 s. Se (average 43 fL) was prepared by passing the solution through an SPG porous

dx.doi.org/10.1021/sb300041z | *ACS Synth. Biol.* 2012, 1, 431–437

membrane (20 μm) (SPG Techno) several times, according to the manufacturer's instructions. GUS and GAL syntheses in emulsions were carried out at 37 °C and monitored using a real-time PCR system (Mx3005P; Agilent). Filter sets used for measuring the fluorescence intensities had excitation/emission wavelengths of 492/516 nm.

Microscopic Observation. Micrographs were obtained using an inverted light microscope (IX70; Olympus) with a 100X oil-immersion objective lens and a digital color CCD camera (VB-7000; Keyence). Bright field images were obtained by differential interference contrast observation. Fluorescence images of were obtained through corresponding filters and dichroic mirror units (NIBA; Olympus).

■ ASSOCIATED CONTENT

Supporting Information

Derivation of the equations and supplementary and supplementary figures. This material is available free of charge via the Internet at http://pubs.acs.org.

■ AUTHOR INFORMATION

Corresponding Author

*Tel: 81-6-6879-4171. Fax: 81-6-6879-7433. E-mail: yomo@ist.osaka-u.ac.jp.

Author Contributions

T.M. and T.Y. conceived the project, K.H. derived the equations, N.I. and H.S. developed w/o emulsion preparation methods, Y.K prepared the IVTT, T.M. performed the experiments, and T.M. and K.H. conducted the analysis. The paper was written by T.M.

Notes

The authors declare no competing financial interest.

■ ACKNOWLEDGMENTS

We would like to thank Ms. Hitomi Komai, Tomomi Sakamoto, and Mizuki Ohzawa for their technical assistance, and Nobuhiko Tokuriki and Casim Sarkar for critical reading of the manuscript. This research was supported in part by the "Global Centers of Excellence Program" of the Ministry of Education, Culture, Sports, Science, and Technology, Japan.

■ ABBREVIATIONS

IVTT, *in vitro* translation and transcription system; GUS, β-glucuronidase; GAL, β-galactosidase

■ REFERENCES

(1) Jorgensen, P., and Tyers, M. (2004) How cells coordinate growth and division. *Curr. Biol. 14*, R1014−1027.

(2) Saucedo, L. J., and Edgar, B. A. (2002) Why size matters: altering cell size. *Curr. Opin. Genet. Dev. 12*, 565−571.

(3) Rafelski, S. M., and Marshall, W. F. (2008) Building the cell: design principles of cellular architecture. *Nat. Rev. Mol. Cell. Biol. 9*, 593−602.

(4) Lizana, L., Konkoli, Z., Bauer, B., Jesorka, A., and Orwar, O. (2009) Controlling chemistry by geometry in nanoscale systems. *Annu. Rev. Phys. Chem. 60*, 449−468.

(5) Klipp, E., Nordlander, B., Kruger, R., Gennemark, P., and Hohmann, S. (2005) Integrative model of the response of yeast to osmotic shock. *Nat. Biotechnol. 23*, 975−982.

(6) Bakal, C., Aach, J., Church, G., and Perrimon, N. (2007) Quantitative morphological signatures define local signaling networks regulating cell morphology. *Science 316*, 1753−1756.

(7) Nalbant, P., Hodgson, L., Kraynov, V., Toutchkine, A., and Hahn, K. M. (2004) Activation of endogenous Cdc42 visualized in living cells. *Science 305*, 1615−1619.

(8) Weart, R. B., Lee, A. H., Chien, A. C., Haeusser, D. P., Hill, N. S., and Levin, P. A. (2007) A metabolic sensor governing cell size in bacteria. *Cell 130*, 335−347.

(9) Meyers, J., Craig, J., and Odde, D. J. (2006) Potential for control of signaling pathways via cell size and shape. *Curr. Biol. 16*, 1685−1693.

(10) Lizana, L., Bauer, B., and Orwar, O. (2008) Controlling the rates of biochemical reactions and signaling networks by shape and volume changes. *Proc. Natl. Acad. Sci. U.S.A. 105*, 4099−4104.

(11) Lang, F., Busch, G. L., Ritter, M., Volkl, H., Waldegger, S., Gulbins, E., and Haussinger, D. (1998) Functional significance of cell volume regulatory mechanisms. *Physiol. Rev. 78*, 247−306.

(12) Hoffman, J. F., and Jamieson, J. D. (1997) *Cell Physiology*, Published for the American Physiological Society by Oxford University Press, New York.

(13) Shimizu, Y., Inoue, A., Tomari, Y., Suzuki, T., Yokogawa, T., Nishikawa, K., and Ueda, T. (2001) Cell-free translation reconstituted with purified components. *Nat. Biotechnol. 19*, 751−755.

(14) Montagne, K., Plasson, R., Sakai, Y., Fujii, T., and Rondelez, Y. (2011) Programming an in vitro DNA oscillator using a molecular networking strategy. *Mol. Syst. Biol. 7*, 466.

(15) Lincoln, T. A., and Joyce, G. F. (2009) Self-sustained replication of an RNA enzyme. *Science 323*, 1229−1232.

(16) Nakajima, M., Imai, K., Ito, H., Nishiwaki, T., Murayama, Y., Iwasaki, H., Oyama, T., and Kondo, T. (2005) Reconstitution of circadian oscillation of cyanobacterial KaiC phosphorylation in vitro. *Science 308*, 414−415.

(17) Walde, P., Goto, A., Monnard, P.-A., Wessicken, M., and Luisi, P. (1994) Oparin's reaction revisited: enzymatic synthesis of poly(Adenyl Acid) in micelles and self-reproducing vesicles. *J. Am. Chem. Soc. 116*, 7541−7547.

(18) Mansy, S. S., Schrum, J. P., Krishnamurthy, M., Tobe, S., Treco, D. A., and Szostak, J. W. (2008) Template-directed synthesis of a genetic polymer in a model protocell. *Nature 454*, 122−125.

(19) Monnard, P. A., Luptak, A., and Deamer, D. W. (2007) Models of primitive cellular life: polymerases and templates in liposomes. *Philos. Trans. R. Soc., B 362*, 1741−1750.

(20) Nomura, S. M., Tsumoto, K., Hamada, T., Akiyoshi, K., Nakatani, Y., and Yoshikawa, K. (2003) Gene expression within cell-sized lipid vesicles. *ChemBioChem 4*, 1172−1175.

(21) Pereira de Souza, T., Steiniger, F., Stano, P., Fahr, A., and Luisi, P. L. (2011) Spontaneous crowding of ribosomes and proteins inside vesicles: A possible mechanism for the origin of cell metabolism. *ChemBioChem*, DOI: 10.1002/cbic.201100306.

(22) Bui, H. T., Umakoshi, H., Ngo, K. X., Nishida, M., Shimanouchi, T., and Kuboi, R. (2008) Liposome membrane itself can affect gene expression in the Escherichia coli cell-free translation system. *Langmuir 24*, 10537−10542.

(23) Noireaux, V., and Libchaber, A. (2004) A vesicle bioreactor as a step toward an artificial cell assembly. *Proc. Natl. Acad. Sci. U.S.A. 101*, 17669−17674.

(24) Sunami, T., Kita, H., Hosoda, K., Matsuura, T., Suzuki, H., and Yomo, T. (2009) Chapter 2 - Detection and analysis of protein synthesis and RNA replication in giant liposomes. *Methods Enzymol. 464*, 19−30.

(25) Kuruma, Y., Nishiyama, K., Shimizu, Y., Muller, M., and Ueda, T. (2005) Development of a minimal cell-free translation system for the synthesis of presecretory and integral membrane proteins. *Biotechnol. Prog. 21*, 1243−1251.

(26) Kita, H., Matsuura, T., Sunami, T., Hosoda, K., Ichihashi, N., Tsukada, K., Urabe, I., and Yomo, T. (2008) Replication of genetic information with self-encoded replicase in liposomes. *ChemBioChem 9*, 2403−2410.

(27) Kurihara, K., Tamura, M., Shohda, K., Toyota, T., Suzuki, K., and Sugawara, T. (2011) Self-reproduction of supramolecular giant

vesicles combined with the amplification of encapsulated DNA. *Nat. Chem. 3*, 775−781.
(28) Doktycz, M. J., and Simpson, M. L. (2007) Nano-enabled synthetic biology. *Mol. Syst. Biol. 3*, 125.
(29) Luisi, P. L., and Stano, P. (2011) Synthetic biology: minimal cell mimicry. *Nat. Chem. 3*, 755−756.
(30) Ichihashi, N., Matsuura, T., Kita, H., Sunami, T., Suzuki, H., and Yomo, T. (2010) Constructing partial models of cells. *Cold Spring Harbor Perspect. Biol. 2*, a004945.
(31) Tawfik, D. S., and Griffiths, A. D. (1998) Man-made cell-like compartments for molecular evolution. *Nat. Biotechnol. 16*, 652−656.
(32) Ghadessy, F. J., Ong, J. L., and Holliger, P. (2001) Directed evolution of polymerase function by compartmentalized self-replication. *Proc. Natl. Acad. Sci. U.S.A. 98*, 4552−4557.
(33) Endo, Y., and Sawasaki, T. (2006) Cell-free expression systems for eukaryotic protein production. *Curr. Opin. Biotechnol. 17*, 373−380.
(34) Yokoyama, S. (2003) Protein expression systems for structural genomics and proteomics. *Curr. Opin. Chem. Biol. 7*, 39−43.
(35) Shimizu, Y., Kanamori, T., and Ueda, T. (2005) Protein synthesis by pure translation systems. *Methods 36*, 299−304.
(36) Jefferson, R. A., Burgess, S. M., and Hirsh, D. (1986) beta-Glucuronidase from Escherichia coli as a gene-fusion marker. *Proc. Natl. Acad. Sci. U.S.A. 83*, 8447−8451.
(37) Lis, J. T., Simon, J. A., and Sutton, C. A. (1983) New heat shock puffs and beta-galactosidase activity resulting from transformation of Drosophila with an hsp70-lacZ hybrid gene. *Cell 35*, 403−410.
(38) Casadaban, M. J., and Cohen, S. N. (1979) Lactose genes fused to exogenous promoters in one step using a Mu-lac bacteriophage: in vivo probe for transcriptional control sequences. *Proc. Natl. Acad. Sci. U.S.A. 76*, 4530−4533.
(39) Jacobson, R. H., Zhang, X. J., DuBose, R. F., and Matthews, B. W. (1994) Three-dimensional structure of beta-galactosidase from E. coli. *Nature 369*, 761−766.
(40) Jain, S., Drendel, W. B., Chen, Z. W., Mathews, F. S., Sly, W. S., and Grubb, J. H. (1996) Structure of human beta-glucuronidase reveals candidate lysosomal targeting and active-site motifs. *Nat. Struct. Biol. 3*, 375−381.
(41) Matsuura, T., Hosoda, K., Ichihashi, N., Kazuta, Y., and Yomo, T. (2011) Kinetic analysis of beta-galactosidase and beta-glucuronidase tetramerization coupled with protein translation. *J. Biol. Chem. 286*, 22028−22034.
(42) Hosoda, K., Sunami, T., Kazuta, Y., Matsuura, T., Suzuki, H., and Yomo, T. (2008) Quantitative study of the structure of multilamellar giant liposomes as a container of protein synthesis reaction. *Langmuir 24*, 13540−13548.
(43) Goodsell, D. S., and Olson, A. J. (2000) Structural symmetry and protein function. *Annu. Rev. Biophys. Biomol. Struct. 29*, 105−153.
(44) Fiordemondo, D., and Stano, P. (2007) Lecithin-based water-in-oil compartments as dividing bioreactors. *ChemBioChem 8*, 1965−1973.
(45) Kato, A., Yanagisawa, M., Sato, Y. T., Fujiwara, K., and Yoshikawa, K. (2012) Cell-Sized confinement in microspheres accelerates the reaction of gene expression. *Sci. Rep. 2*, 283.
(46) Pohorille, A., and Deamer, D. (2002) Artificial cells: prospects for biotechnology. *Trends Biotechnol 20*, 123−128.
(47) Rasmussen, S., Chen, L., Deamer, D., Krakauer, D. C., Packard, N. H., Stadler, P. F., and Bedau, M. A. (2004) Evolution. Transitions from nonliving to living matter. *Science 303*, 963−965.
(48) Szostak, J. W., Bartel, D. P., and Luisi, P. L. (2001) Synthesizing life. *Nature 409*, 387−390.
(49) Matsuura, T., Kazuta, Y., Aita, T., Adachi, J., and Yomo, T. (2009) Quantifying epistatic interactions among the components constituting the protein translation system. *Mol. Syst. Biol. 5*, 297.
(50) Kazuta, Y., Adachi, J., Matsuura, T., Ono, N., Mori, H., and Yomo, T. (2008) Comprehensive analysis of the effects of Escherichia coli ORFs on protein translation reaction. *Mol. Cell. Proteomics 7*, 1530−1540.